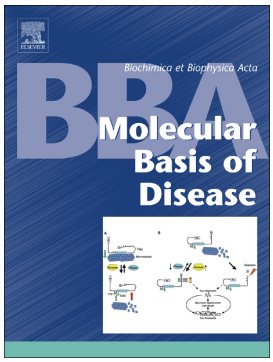

Deficiency of CD73 activity promotes protective cardiac immunity against Trypanosoma cruzi infection but permissive environment in visceral adipose tissue

Natalia Eberhardt, Liliana Maria Sanmarco, Gastón Bergero, Martín Gustavo Theumer, Mónica Cristina García, Nicolas Eric Ponce, Roxana Carolina Cano, Maria Pilar Aoki

PII: S0925-4439(19)30315-1

DOI: https://doi.org/10.1016/j.bbadis.2019.165592

Reference: BBADIS 165592

To appear in: *BBA - Molecular Basis of Disease*

Received date: 14 May 2019

Revised date: 16 September 2019

Accepted date: 25 September 2019

Please cite this article as: N. Eberhardt, L.M. Sanmarco, G. Bergero, et al., Deficiency of CD73 activity promotes protective cardiac immunity against Trypanosoma cruzi infection but permissive environment in visceral adipose tissue, *BBA - Molecular Basis of Disease*(2019), https://doi.org/10.1016/j.bbadis.2019.165592

Deficiency of CD73 activity promotes protective cardiac immunity against *Trypanosoma cruzi* infection but permissive environment in visceral adipose tissue

Running title: *CD73 modulates immune response in a tissue-dependent manner.*

Natalia Eberhardt [a b]; Liliana Maria Sanmarco [a b 1]; Gastón Bergero [a b]; Martín Gustavo Theumer [a b]; Mónica Cristina García [c]; Nicolas Eric Ponce [a]; Roxana Carolina Cano [b d]; Maria Pilar Aoki [a b]

E-mails: neberhardt@fcq.unc.edu.ar; lsanmarco@bwh.harvard.edu; gbergero@fcq.unc.edu.ar; mgtheumer@fcq.unc.edu.ar; mgarciasotelo@gmail.com; nponce@fcq.unc.edu.ar; rcano@fcq.unc.edu.ar; paoki@fcq.unc.edu.ar

[a] Centro de Investigaciones en Bioquímica Clínica e Inmunología (CIBICI), Consejo Nacional de Investigaciones Científicas y Tecnológicas (CONICET), Córdoba, Argentina.

[b] Departamento de Bioquímica Clínica, Facultad de Ciencias Químicas, Universidad Nacional de Córdoba, Córdoba, Argentina.

[c] Unidad de Tecnología Farmacéutica (UNITEFA), Consejo Nacional de Investigaciones Científicas y Tecnológicas (CONICET), Departamento de Ciencias Farmacéuticas, Facultad de Ciencias Químicas, Universidad Nacional de Córdoba, Córdoba, Argentina.

[d] Unidad Asociada Área Ciencias Agrarias, Ingeniería, Ciencias Biológicas y de la Salud, Consejo Nacional de Investigaciones Científicas y Tecnológicas (CONICET), Facultad de Ciencias Químicas, Universidad Católica de Córdoba, Córdoba, Argentina.

[1] Ann Romney Center for Neurologic Diseases, Brigham and Women's Hospital. Harvard Medical School, Boston, MA, United States (present address).

Corresponding author: Maria Pilar Aoki

Address: Haya de la Torre and Medina Allende. Ciudad Universitaria. CP 5000. Córdoba. Argentina. Tel: +54-351-5353851 ext 3181. Fax: +54-351-4333048 ext 3177. E-mail: *paoki@fcq.unc.edu.ar*

Abstract

Damaged cells release the pro-inflammatory signal ATP, which is degraded by the ectonucleotidases CD39 and CD73 to the anti-inflammatory mediator adenosine (ADO). The balance between ATP/ADO is known to determine the outcome of inflammation/infection. However, modulation of the local immune response in different tissues due to changes in the balance of purinergic metabolites has yet to be investigated. Here, we explored the contribution of CD73-derived ADO on the acute immune response against *Trypanosoma cruzi* parasite, which invades and proliferates within different target tissues. Deficiency of CD73 activity led to an enhanced cardiac microbicidal immune response with an augmented frequency of macrophages with inflammatory phenotype and increased CD8+ T cell effector functions. The increment of local inducible nitric oxide (NO) synthase $(iNOS)^{+}$ macrophages and the consequent rise of myocardial NO production in association with reduced ADO levels induced protection against *T. cruzi* infection as observed by the diminished cardiac parasite burden compared to their wild-type (WT) counterpart. Unexpectedly, parasitemia was substantially raised in CD73KO mice in comparison with WT mice, suggesting the existence of tissue reservoir/s outside myocardium. Indeed, CD73KO liver and visceral adipose tissue (VAT) showed increased parasite burden associated with a reduced ATP/ADO ratio and the lack of substantial microbicidal immune response. These data reveal that the purinergic system has a tissue-dependent impact on the host immune response against *T. cruzi* infection.

KEYWORDS:

CD73; CD39; Extracellular ATP; Adenosine; Chagas disease; Purinergic signaling

1. Introduction

The purinergic system has taken on a robust significance as a central signaling pathway for immune response modulation. It involves a wide range of metabolites, among which the purine nucleotide ATP and the nucleoside adenosine (ADO) act as immunostimulatory or immunosuppressive signals, respectively, influencing the outcome of the host response to several stimuli [1]. In steady state, ATP is almost exclusively found in the intracellular compartment, reaching millimolar concentrations, but upon infection-induced inflammation ATP is released to the extracellular milieu where it acts as a potent immune signaling molecule [2]. In contrast, extracellular ADO represents a regulatory feedback mechanism that limits tissue injury by counteracting the pro-inflammatory actions of ATP. Due to its compensatory effects, extracellular ADO has been progressively recognized as a retaliatory metabolite that promotes tissue homeostasis but also counteracts microbicidal responses [3]. ADO accumulates in inflamed and hypoxic tissues by mean of the action of two ectoenzymes: ecto-apyrase (CD39) that mediates the dephosphorylation of ATP to ADP and then to AMP, and ecto-5'-nucleotidase (CD73), which catalyzes the final reaction to convert AMP to ADO [4]. Although the loss of the balance between extracellular ATP and ADO are known to trigger several pathological effects in cancer [5-8], infectious [9-13] and autoimmune diseases [14, 15]; few studies have addressed the impact of purinergic system imbalance on the pathophysiology of Chagas disease.

Trypanosoma cruzi infection leads to the development of chronic Chagas cardiomyopathy, a potentially lethal illness which eventually requires cardiac transplantation. During the acute phase of infection, parasites replicate within different tissues showing a strong tropism for the myocardium. Innate and adaptive

immune responses control parasitemia but are insufficient to totally clear the infection, and most individuals remain infected for life. The persistence of the parasite within target tissues triggers activation and recruitment of monocytes (Mo)/macrophages which represent the early line of defense against the parasite and determine, at least in part, the development of adaptive immunity [16]. Inflammatory or classically activated macrophages (M1 subset) are essential for the control of the infection as they produce nitric oxide (NO), a crucial antimicrobial metabolite that arrests parasite growth and M1 cytokines such as IL-12 and TNF, which induces the production of IFN-γ and the development of Th1-dependent $CD8^+$ T cell response. Increasing evidence demonstrates that ADO deactivates macrophage microbicidal mechanisms [17] promoting alternative macrophage profile (M2 subset) [18]. We have recently reported that transient pharmacologic inhibition of CD73 activity in *T. cruzi*-infected BALB/c mice improves the outcome of Chagas cardiomyopathy by preventing the M1 to M2 macrophages shift within infected myocardium, enhancing the production of NO and pro-inflammatory cytokines which led to decrease local parasite burden [19]. These findings strongly suggest that the modulation of purinergic signals influence the outcome of this cardiovascular disease.

As a logical consequence of cardiac cell tropism, experimental models of *T. cruzi* infection have served as an invaluable tool to study the immune response triggered by the myocardium to microbial [19-25]. However, *T. cruzi* residence is not restricted to cardiac tissue. Indeed, the parasite has been detected in a wide range of other reservoirs, such as liver and visceral adipose tissue (VAT) [26]. Cumulative evidence suggests that VAT is an essential niche for parasite persistence because it can serve as an enriched nutrient reservoir, where the parasite can persist in quiescent state avoiding immune response [27, 28]. However, the mediators

involved in the unresponsiveness of the local immune system are largely unknown. In the present study, we examined how the deficiency of CD73 enzymatic activity modulates the immune response to *Trypanosoma cruzi* and, in consequence, parasite persistence in different infection target tissues.

2. Materials and methods

Ethics statement

All animal experiments were carried out with approval of the animal handling and experimental procedures by the Institutional Committee for the Care and Use of Laboratory Animals (CICUAL- Res:736/2018) of CIBICI-CONICET, Facultad de Ciencias Químicas, Universidad Nacional de Córdoba, Córdoba, Argentina in strict accordance with the recommendation of the U.S Department of Health and Human Services Guide for the Care and Use of Laboratory Animals.

Mice

C57BL/6J (WT) mice were obtained from Facultad de Ciencias Veterinarias, Universidad Nacional de La Plata, Argentina. CD73-deficient mice (CD73KO B6.129S1-Nt5e^{tm1Lft}/J - JAX stock #018986) were purchased at The Jackson Laboratories (USA) [29]. Mice were housed in the Animal Facility of Facultad de Ciencias Químicas, Universidad Nacional de Córdoba OLAW-NIH assurance number F16-00193 (A5802-01). The animals had *ad libitum* access to water and feed in all experiments carried out. Mice were anesthetized with isoflurane.

Parasites and experimental infection

Six to eight week-old male and female mice were infected intraperitoneally (i.p) with 1000 blood-derived trypomastigotes of *T. cruzi* (Tulahuen strain). Non-infected mice were used as control. Bloodstream trypomastigote forms were harvested by heart puncture from anesthetized infected mice and were maintained for successive passages. Parasitemia was counted by using a Neubauer's chamber in whole blood. Mouse survival was followed every day until 60 days post-infection (dpi).

Histological analysis

Visceral adipose tissues were fixed in 10% buffered formalin and embedded in paraffin for hematoxylin/eosin (H&E) stain. Five-micron-thick sections were examined by light microscopy Nikon Eclipse TE 2000 U equipped with a digital video camera. The quantification analysis of histomorphometry of visceral adipose tissue was performed using ImageJ image analysis software with "Measure and Label Macro" plugin [30].

Immunofluorescence

Tissue samples (heart, VAT and liver) from infected WT mice were collected at 7 dpi, placed in formalin-PBS 10% overnight and then, washed with PBS and stored at 4°C in sucrose 30%-PBS until cryostat sectioning. The samples were covered with OCT and sectioned at 5-7 µm in a Cryotome 0620E (Thermo Scientific®). The slides were fixed in cold acetone for 10 minutes, blocked with BSA 5%-PBS and labeled with anti-CD73 rabbit primary antibody (Abcam®) and then with Alexa 555 anti-rabbit IgG secondary antibody for 60 min, the cell nuclei were stained with Hoescht. The images were obtained with FLUOVIEW FV1200 Olympus confocal microscope. The mean fluorescence intensity (MFI)/cell was quantified in 10 High Power Fields (HPF) (60x objective lens with 4X digital zoom) by making a Z-projection of the stacks of confocal images and analyzing the mean grey value of the regions of interest (ROIs) using Image J software. The fluorescence given by the secondary antibody and by the tissue autofluorescence was subtracted using appropriate controls.

Isolation of hepatic leukocytes

Hepatic immune cells were isolated from all mouse groups as described previously [31]. Briefly, livers were obtained in PBS (Gibco®) and passed through 100 mm nylon meshes, erythrocytes were removed using lysis buffer (Gibco®). Hepatocytes were separated from immune cell by a 35% and 70% bilayer Percoll gradient (GE

Healthcare®) and living cells were counted with Trypan blue in a Neubauer's chamber and stained for flow cytometry.

Isolation of cardiac immune cells

The isolation protocol of heart leukocytes was carried out as described in Ponce *et al* (19). At indicated time-points, infected hearts were perfused with PBS (Gibco®), weighed and disaggregated mechanically and enzymatically with 0.25% trypsin solution (Sigma®). The digested tissue was gently pressed through a cell strainer (70 μm; BD Falcon). Mononuclear cells and granulocytes were isolated by 35% and 70% bilayer Percoll density gradient centrifugation (GE Healthcare®). Viable cell counting was determined by Trypan Blue exclusion using a Neubauer's chamber and stained for flow cytometry.

Stromal vascular fraction (SVF) cells isolation from visceral adipose tissue

Wet-tissue weights were taken immediately after removal of VAT depots using an analytical balance. Then, the specimens were minced and digested for 45 min at 37°C with type 2 collagenase (0.8 mg/mL; Sigma) in Hanks' Balanced Salt solution buffer allowing the isolation of SVF. After the addition of Hanks supplemented with 10% FBS and filtration of the digested tissue through cell strainer (70 μm; BD Falcon), the filtrate was centrifuged at 1800 rpm. The SVF was obtained from the resulting supernatant, subsequently stained and analyzed by flow cytometry.

Flow cytometry analysis

Peripheral blood was stained with the following antibodies: anti-mouse APC-CD11b, PECy7-Ly6C, PerCP/Cy5.5-CD73 and biotin-CD39. Then, cells were incubated with FITC-streptavidin for 15 min and incubated with lysis buffer (Gibco®) to lyse red blood cells. Tissue cell suspensions were stained for flow cytometry with the following

antibodies: rat monoclonal anti-mouse APC-CD45, PE-F4/80, PECy7-F4/80, APCCy7-CD86, PECy7-CD206, FITC-CD3, PE-CD8 and APCCy7-CD4, PECy7-Ly6C, APCCy7-Ly6G, FITC-CD19, PerCP-eFluor-CD39 and rabbit polyclonal anti-mousse CD73 (rabbit) (BioLegend®, BD Pharmingen®, eBioscience® and Abcam®). Finally, cells were washed and incubated with anti-rabbit Alexa Fluor 488 or Alexa 647 for 15 min. To evaluate the intracellular cytokines and enzymes expression, samples were treated with Golgi Stop/Golgi Plug at 37˚C for 4 h, fixed and permeabilized with BD Cytofix/Cytoperm and Perm/Wash (BD Biosciences) according to the manufacturer's instruction. Afterwards, cells were incubated with the following antibodies: monoclonal anti-mouse APC-IL-10, PerCP/Cy5.5-IFN-γ, APC-IL-12, FITC-CD107a, PE-Arginase-1 (R&D), rabbit monoclonal anti-mouse iNOS/NOS Type II (eBioscience, BD Pharmingen, and BioLegend). Finally, cells were washed and incubated with anti-rabbit Alexa Fluor 488 or Alexa 647 for 15 min. Stained samples were acquired using a FACS Canto II cytometer (Becton Dickinson) and data were analyzed using FlowJo software 10 (Tree Star, Inc.).

Parasite burden by PCR assay

To determine tissue parasitism, genomic DNA was purified from infected heart, liver and VAT at different times post-infection using TRIzol reagent and following the manufacturer's instructions. Satellite DNA from *T. cruzi* was quantified by real time PCR using specific Custom Taqman Gene Expression Assay (Applied Biosystem®) [32]. A sample containing 2 μg of genomic DNA was amplified. Abundance of satellite DNA from *T. cruzi* was normalized to GAPDH (Taqman Rodent GAPDH Control Reagent, Applied Biosystem®) or 18S abundance (Eukaryotic 18S rRNA Endogenous Control, Applied Biosystems®) and expressed as arbitrary units (AU).

Cytokine and chemokine measurements

At indicated time points, hearts were perfused and disaggregated in RIPA buffer. ELISA sandwich was performed for the quantification of IL-17A, IL-4, IL-10, TNF, IL-1β, IL-6, IFN-γ and IL-12 levels in CD73KO and WT mice. Briefly, ELISA plates were coated with anti-cytokine antibodies (BD Pharmingen® and e-Bioscience®) overnight, then washed with PBS/Tween 0.05% and blocked with albumin for 1 h. Standard curves were generated using recombinant cytokines (BD Pharmingen® and e-Bioscience®). Samples and standard cytokines were incubated overnight at 4 ºC. After washing, the plates were incubated with biotinylated anti-cytokine antibody (BD Pharmingen® and e-Bioscience®) for 1 h at room temperature and then, previously washed, streptavidin-peroxidase (BD Pharmingen®) was added for 30 min. The reaction was revealed using TMB Substrate Chromogen (Dako®), before being read at 450 nm in a microplate reader (BioTek). The total protein concentration of heart samples was determined by the Bradford method (Bio-Rad). Data were expressed as the mean of ratio between pg or ng of cytokine per mg of total heart protein. Plasma samples were sent to Biocon Laboratory (Córdoba, Argentina) to measure ALT (alanine aminotransferase), AST (aspartate aminotransferase), total creatine kinase (CK), CK-MB isozyme as biochemical markers of liver and heart tissue damage.

Nitric oxide measurement

Nitrite levels were measured spectrophotometrically by Griess reaction to quantify the amount of NO in plasma and tissue lysates in RIPA buffer. Briefly, 30 µL of Griess reagent (Sigma Aldrich®) that converts nitrates to nitrites was added to 30 µL of plasma/tissue lysates, and absorbance was read after 15 min at 540 nm using an automated plate reader (BioTek). A $NaNO_2$ standard curve was performed to calculate the nitrite concentration. In parallel, the total protein concentration of heart samples was determined by the Bradford method (Bio-Rad).

ATP assay

To measure the extracellular ATP levels released by infected target tissues, heart, liver and VAT explants were perfused and weighted right after mice sacrifice. The specimens were washed three times and incubated for 1 h at 37°C in sterile PBS (Gibco®) supplemented with antibiotics (10). ATP levels were quantified in the supernatants of each organ and in plasma samples by ATP Determination Kit (Invitrogen™), according to the manufacturer's instructions. Briefly, samples were incubated with luminescent reaction mix at room temperature for 15 min in a 96-well black plate protected from light. Luminescence was measured at 560 nm in a Synergy 2 Multi-Mode Reader (BioTek). A standard curve was plotted to calculate the ATP concentration and a regression analysis was applied as indicated by the kit manufacturer.

Measurement of ADO levels by high-performance liquid chromatography (HPLC)

ADO released in the supernatant of infected tissues was determined by HPLC analysis. The analytical quantification of ADO in the samples was performed using Agilent HP 1220 HPLC system equipped with an isocratic pump and a variable wavelength detector at 257 nm, with data acquisition and processing being performed using Agilent BootP software. Chromatographic separations were carried out using a Phenomenex® C18 reverse phase column (150 x 4.6 mm, 5 µm particle size). Analysis was performed with 0.4% phosphoric acid: methanol (95:5, v/v) as the mobile phase at a flow-rate of 0.8 mL/min in the isocratic mode. For analysis, 10 µL of each sample were injected, and the run time was set at 10 min. All solutions were filtered through 0.45 µm cellulose filters (Millipore®) and then quantified by HPLC. ADO peak areas were confirmed by the co-injection of internal standard together with the analyzed samples and were used for quantitative analysis. ADO levels in the biological samples were quantified by relating the analytical peak area to the regression line of calibration curve.

For the calibration curve, a stock solution of 500 µM ADO standard (Sigma-Aldrich®) in distillated water was prepared. Subsequently, six-point calibration curve were prepared over a range of 0.1 to 100 µM by diluting several milliliters of stock solution with PBS (Gibco®). These solutions were prepared in triplicate. The calibration curve was constructed by plotting the mean peak area of ADO *vs* ADO concentration.

For method validation the following criteria were evaluated: linearity, accuracy, precision, limit of detection (LOD), lower limit of quantitation (LLOQ) and stability following the instructions of Bioanalytical method validation- Guidance for Industry from U.S Food and Drug Administration. The validation parameters are depicted in Table I.

Table I. Parameters of the HPLC bioanalytical method for quantification of ADO.

Parameters	**Results**
Linearity (n=6)	
Concentration range [µM]	0.1-100
Correlation coefficient [r^2]	1.000
Equation	$y = 17.68x + 0.35$
LOD [µM]	0.05
LLOQ [µM]	0.1
Precision, %CV	12.44 ± 1,28 %
Accuracy, % E_R	3.70 ± 0.85 %
Stability, %S *Freeze/thaw (1 cycle)*	98.96 ± 6.21 %

LOD: limit of detection, LLOQ: lower limit of quantitation, %CV: coefficient of variation, %E_R: inaccuracy. For %CV, %E_R and %S the values reported correspond to the Mean± DS% from Lower concentration [ADO]= *0.1 µM*; Mid concentration [ADO]=*5 µM* and Higher concentration [ADO]=*100 µM*.

The range of linearity was established based on three separate assay runs of freshly prepared calibration standards and it was assessed by determining coefficient of correlation (r^2) and slope using linear regression analysis. The accuracy and precision of the method was performed using 15 standard samples at three concentrations (100, 5

and 0.1 μM) analyzed over three consecutive days to determine intra e inter-day variations.

Statistical analysis

Statistical significance of comparisons of mean values was assessed by a two-tailed Student's t-test for comparison between two groups. To compare different groups of experimental conditions, an ANOVA (two-way or one-way ANOVA) and the Bonferroni or Tukey post hoc test were performed. A p-value < 0.05 was considered significant (* $p < 0.05$; ** $p < 0.01$; *** $p < 0.001$; ns: non-significant; ND: non-detectable).

3. Results

Infected CD73-deficient mice mounted acute effective cardiac microbicidal response associated to local parasite burden reduction

To assess how the absence of CD73 enzymatic activity modulates cardiac immune response to *T. cruzi* infection, we first comparatively analyzed the kinetics of leukocytes and macrophage profiles within infected CD73KO myocardium following the gate strategy depicted in Fig. 1A. Regarding the frequency of cardiac leukocytes ($CD45^+$), macrophages ($F4/80^+$) were the most frequent population at early times post-infection (7 dpi), which showed a higher frequency in CD73KO mice compared to WT mice ($p<0.01$). Macrophages progressively decreased, whereas the number of T lymphocytes (CD3+) increased later in the acute phase (21 dpi) in both mouse strains. Neutrophil frequency also diminished from 7 dpi to 21 dpi in CD73KO animals, but not in WT animals (Fig. 1B). The number of leukocytes in CD73KO-infected hearts progressively increased and peaked at 21 dpi (Fig S1A). No differences were observed in the absolute number of cardiac leukocytes in both WT and CD73KO mice at 21 dpi (Fig. S1A). To further establish the kinetics of cardiac macrophage subsets, we analyzed the relative percentage of inflammatory/M1-like macrophages ($CD45^+$ $F4/80^+$ $CD86^+$ $CD206^-$) and anti-inflammatory/M2-like macrophages ($CD45^+$ $F4/80^+$ $CD86^-$ $CD206^+$) throughout the infection. In the peak of inflammatory infiltrate (21 dpi), while WT mice presented a majority of cardiac M2-like macrophages ($p <0.001$), CD73KO hearts showed a predominance of M1-like macrophages over the M2-like subset ($p <0.01$). Likewise, the frequency of cardiac M1-like macrophages were increased while the percentage of macrophages with M2-phenotype were diminished in CD73-deficient mice compared to WT mice (Fig. 1C). We have previously reported that, independent of the WT mouse strain, immediately after *T. cruzi* infection (4 dpi), the percentage of macrophages with

M1/inflammatory phenotype predominated over the M2 macrophages subset but, as soon as 7 dpi, the M1-like population decreased while the M2-like subset strongly increased and remained sustained throughout the acute and chronic phase of the infection [19, 23]. In contrast, here we observed that in infected CD73KO mice, the percentage and the absolute number of cardiac M1-like macrophages predominated over the M2 phenotype during the entire acute phase (Fig. 1D). These results are in line with our previous report indicating that pharmacologic inhibition of CD73 activity prevents the switch from M1 toward M2 phenotype in the early acute phase of infection [19]. Since M1 macrophages exert their anti-microbial activity through the production of NO a potent microbicidal metabolite [33], we next investigated NO levels in infected heart tissues. Coincident with the raise in the amount of macrophages in CD73KO mice, cardiac NO levels significantly increased at 21 dpi compared to WT mice (Fig. 1E). In line with this observation, the frequency of $iNOS^+$ M1-like macrophages was remarkably increased in CD73KO heart tissue in comparison with WT at this time point (Fig. 1F). Furthermore, IL-12 production by M1-like macrophage population was higher in CD73KO hearts. In contrast, the percentage of arginase-1 $(Arg\text{-}1)^+$ and $IL\text{-}10^+$ M2-like macrophages diminished in deficient heart tissues compared to WT, while no differences were observed in IL-10 expression per cell (MFI) in both studied groups (Fig. 1G). Considering that CD73KO mice showed a marked deviation towards M1 macrophage phenotype, it is plausible to think that the adaptive immune response could also be derived towards a robust cytotoxic T-cell phenotype. In this sense, we found that cardiac $CD8^+$ T lymphocytes from CD73KO mice showed augmented frequency of IFN-γ^+ and $CD107a^+$ cells, accompanied by an increased CD107a MFI in comparison with the WT counterpart but no differences were observed in IFN-γ MFI between both groups (Fig. 1H).

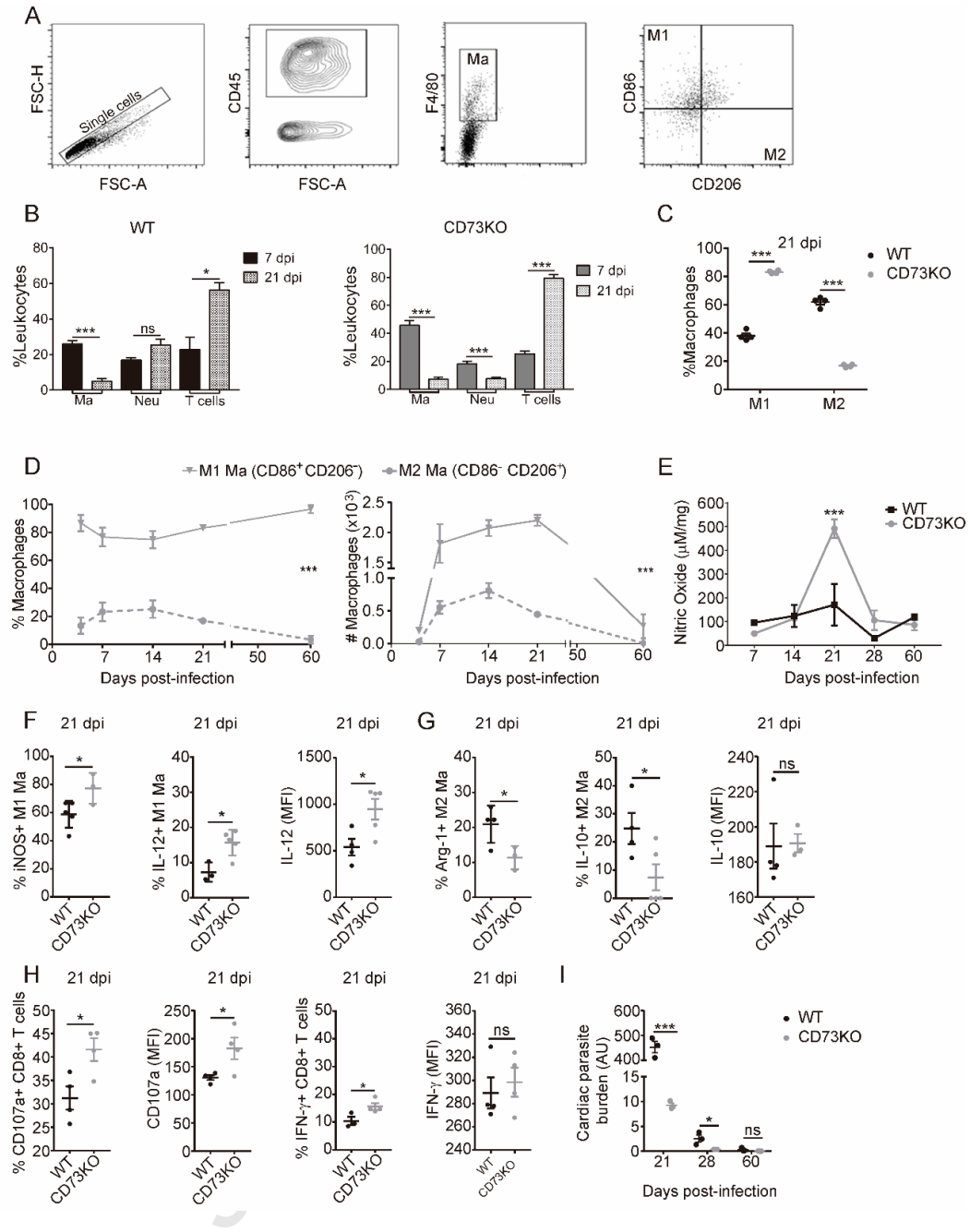

Figure 1. Infected CD73-deficient mice developed a cardiac microbicidal response associated with a reduction in the local parasite burden. (A) Flow cytometry gating strategy. After exclusion of doublets and debris by using forward light scatter-height (FSC-H) vs. forward light scatter-area (FSC-A) density dot plots; leukocytes were gated according to CD45+ staining and macrophages (Ma) were selected by their F4/80$^+$ expression. Ma subpopulations were evaluated based on the expression of CD206 and CD86. (B) Percentage of macrophages (Ma), neutrophils (Neu) and T lymphocytes (T cells) in WT (left) and CD73KO (right) cardiac tissue at different time points (n=5). Statistical analysis comparing 7 *vs*. 21 dpi in each subpopulation is depicted. (C) Frequency of cardiac M1-like and M2-like Ma in WT (n=4) and CD73KO mice (n= 5) at 21 dpi. (D) Relative percentage and absolute number kinetics of Ma with M1 and M2 phenotype in CD73KO infected hearts. Percentages are expressed as the relationship between both single positive populations. (E) Kinetics of cardiac NO levels measured by Griess reagent in infected WT (black line) and CD73KO (grey line) mice. (F) Frequency of iNOS$^+$ and IL-12$^+$ Ma gated into M1 phenotype (n=4-5). MFI of IL-12$^+$ gated in M1 Ma (n=4-5). (G) Frequency of Arg-1$^+$ and IL-10$^+$ M2-like Ma (n=3-5) and MFI of IL-10 expression on M2 Ma (n=4-5). (H) Frequencies and MFI of IFN-γ and

CD107a expression in $CD8^+$ CD3+ cells (n=4); (F-H) the assays were comparative between WT and CD73KO hearts at 21 dpi. (I) Quantitative assessment of cardiac parasite load by real-time PCR (n=3-5). The results are mean ± SEM of at least two independent experiments. (* $p < 0.05$; ** $p < 0.01$; *** $p < 0.001$; ns: non-significant).

Considering that cytokines play an important role in orchestrating the intrinsic cardiac stress response and that they are important candidates for the local activation of macrophages within the myocardium, we aimed to characterize the kinetics of cardiac cytokines in the altered purinergic environment (Figure 2A). Inflammatory cytokines such as TNF, IL-17 and IL-1β peaked at 21 dpi, while IL-12 levels, the cytokine responsible of M1-biased phenotype, remained increased between 14 and 28 dpi compared to non-infected basal conditions. Likewise, TNF, IL1-β and IL-6 were increased at 21 dpi in CD73-deficient heart compared to WT hearts. Furthermore, IL-6 also augmented at 21 dpi in infected CD73KO mice compared to non-infected mice. Strikingly, two peaks of IFN-γ were observed at early times after infection (4 dpi) and later on the acute phase (21 dpi) in CD73-deficient hearts compared to basal conditions. Moreover, IFN-γ was also significantly increased at 4 dpi compared to WT counterpart. IL-4, a M2 macrophage-associated cytokine, remained constant in CD73KO hearts in the period of time evaluated, with higher levels at 4 dpi than the WT counterpart. Coincident with the macrophage switch towards an M2-like phenotype in WT cardiac tissue described in Figure 1C, IL-4 diminished at 4 dpi ($p<0.05$ vs not infected) but substantially increased at 7 dpi in WT-infected hearts ($p<0.05$ vs 4 dpi), suggesting that IL-4 augmented levels could be triggering the switch toward M2-like macrophages in these animals. The anti-inflammatory IL-10 showed a significant increase in the first period after infection compared to non-infected condition (4 and 7 dpi) in both mice strains (Fig. 2A). The results suggest that CD73 activity abrogation promotes the inflammatory/microbicidal phenotype of macrophages with the consequent deviation towards an active adaptive immune response. In accordance with these observations,

cardiac parasite load was significantly diminished at 21 and 28 dpi in CD73KO mice compared to WT mice (Fig. 1I) reinforcing the idea that abrogation of CD73-derived ADO fuels the acute eradication of parasites by promoting a microbicidal milieu in cardiac tissue. Nevertheless, no significant differences were found in total creatine kinase (CK) and CK-MB iso-enzyme levels (Fig. S1B), suggesting that both groups of mice undergo comparable myocardial damage.

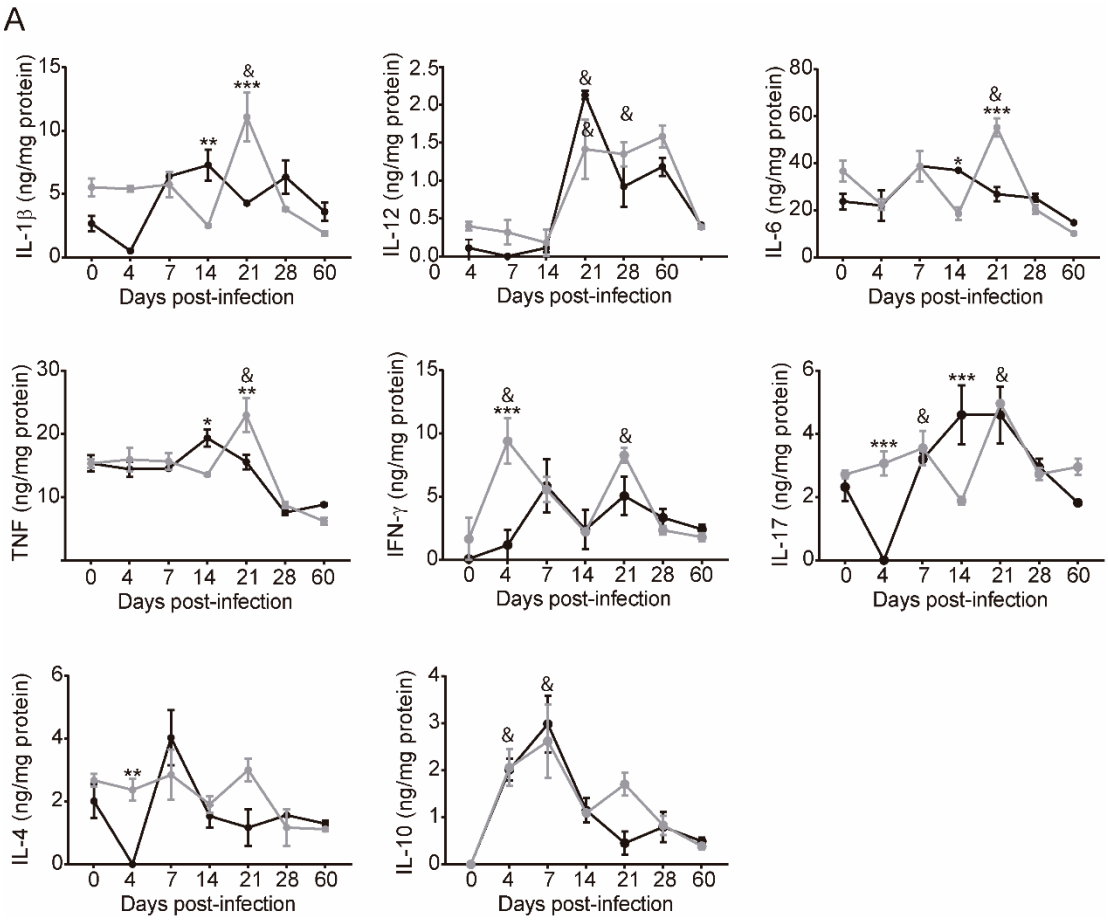

Figure 2. CD73KO heart tissue had a predominant inflammatory cytokine microenvironment. (A) Kinetics of cardiac cytokines normalized to milligram of heart protein in CD73KO mice (grey lines) compared to WT mice (black lines). Statistical analysis was applied compared to NI (non-infected) animals (& $p < 0.05$ NI).

CD73-deficiency augmented circulating inflammatory monocytes but failed to control parasitemia

Considering that recruited Ly6C^{hi} Mo could be the source of inflammatory macrophages (20), we evaluated whether the deficiency of CD73 activity could be modulating

circulating Mo subsets. Peripheral blood of CD73-deficient mice exhibited significant increased frequency of $CD11b^{+}$ $Ly6C^{hi}$ Mo at early times post-infection (7 dpi), even though the majority of circulating Mo belong to patrolling subset ($CD11b^{+}$ $Ly6C^{low}$) in both groups of mice. While no differences were observed at 14 dpi, the ratio reverted at 21 dpi when WT animals show higher percentage of inflammatory Mo compared to CD73KO mice (Fig. 3A). No differences were observed in the frequencies of NO^{+} Mo in both groups of mice at 21 dpi (data not shown).

To determine whether *T. cruzi* infection modulated circulating ATP levels, we comparatively measured plasma levels at different time points. No differences were found in plasma ATP levels from CD73-deficient mice before and after infection. However, these levels decreased in WT mice at 7 dpi and no differences were observed at 14 and 21 dpi compared with those non-infected (Fig. 3B). The expression of both ectoenzymes increased in inflammatory Mo subpopulation in infected compared to non-infected WT animals (Fig. 3C).

Quite unexpectedly, CD73KO mice exhibited a higher parasitemia at 14 and 21 dpi than WT mice (Fig. 3D), which inversely correlated with plasma NO levels (Fig. 3E). Considering the frequency of circulating leukocytes, the reduction of cardiac parasite load and increased parasitemia, the overall data suggested that *T. cruzi* could be invading and replicating in other host reservoirs.

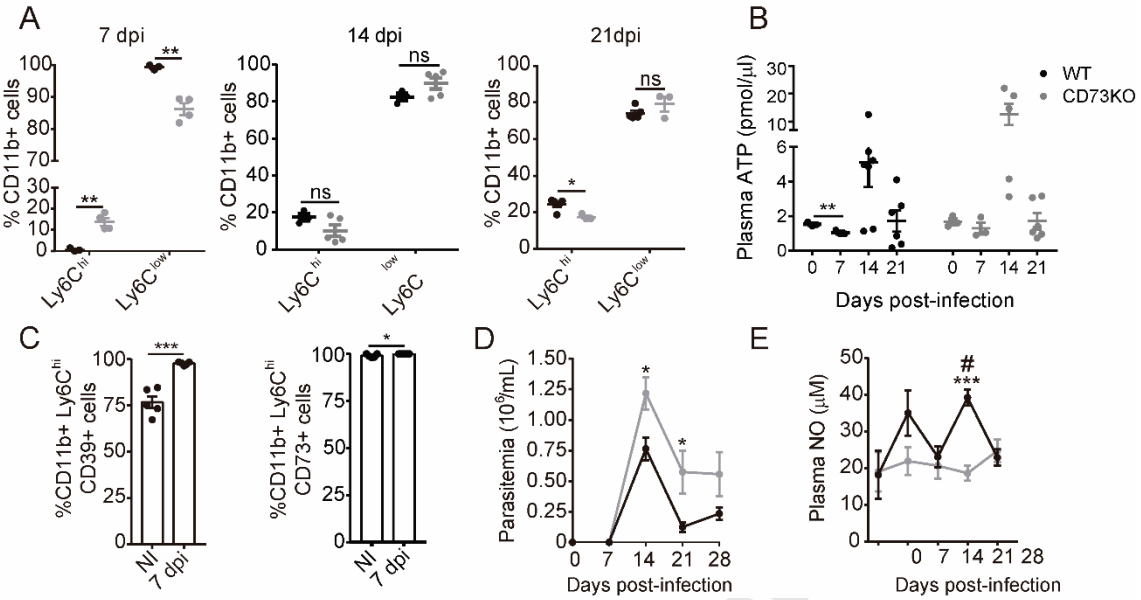

Figure 3. Deficiency of CD73 raised circulating inflammatory monocytes but failed to control parasitemia. (A) Percentage of inflammatory (CD11b^{+} Ly6C^{hi}) and patrolling (CD11b^{+} Ly6C ^{low}) Mo in peripheral blood of infected WT (black) and CD73KO (grey) mice (n=4) (7, 14 and 21 dpi). (B) Kinetics of plasma levels of ATP (pmol/µl) measured in CD73KO and WT mice. (C) Frequencies of CD73^{+} and CD39^{+} inflammatory Mo in peripheral blood from non-infected (NI) and infected (7 dpi) WT mice (n=5). (D) Parasitemia kinetics (10^{6} parasites/mL) (n=4-6). Representative assay of three independent experiments. (E) Plasma NO levels measured by Griess Reagent in infected mice (n=3-4 animals per group). The results are expressed as mean ± SEM of a representative assay of at least two independent experiments if not indicated otherwise (* $p < 0.05$; ** $p < 0.01$; *** $p < 0.001$; ns: non-significant).

Deficiency of CD73 activity was associated to increased VAT parasite burden

Considering that VAT serves as a reservoir, in which the parasite evades the microbicidal host immune response [34], we next investigated the impact of CD73-derived ADO in VAT tissue. Strikingly, CD73KO mice exhibited a significant increase in VAT/body weight ratio at basal condition, without significant differences in adipocyte size and area compared to WT mice (Fig. 4B). Thus, it is plausible to think that the greater VAT/body weight ratio in deficient mice made them more susceptible to host the parasite. Indeed, higher parasite load was found in VAT from CD73KO than WT mice at 21 and 28 dpi (Fig. 4C). In both group of mice, VAT/body weight ratio diminished at 21 dpi compared to non-infected condition (Fig. 4A), but at 60 dpi, when the chronic phase is beginning, the ratio was restored up to similar values to non-

infected mice and the local parasite load decreased to almost undetectable levels (Fig. 4C).

When evaluating local immune response at 21 dpi, we found that there were no differences in the absolute number of infiltrating leukocytes or macrophages comparing both groups of mice (Fig. 4D-E). Moreover, the frequency of M1-like or M2-like polarized macrophages (Fig. 4F) as well as the percentage of $iNOS^+$ macrophages and the local NO levels were also similar between both groups (Fig. 4G). Strikingly, the frequency of M1-like macrophages was lower than M2-like macrophages in infected VAT from both mouse strains. Only the frequency of Arg-1^+ M2-like macrophages in CD73KO VAT was increased compared to WT VAT (Fig. 4H). Furthermore, no differences were observed in the production of CD107a nor IFN-γ in $CD8^+$ T lymphocytes (Fig. 4I). Our results demonstrate that CD73 enzymatic deficiency does not potentiate the anti-*T. cruzi* immune response in VAT.

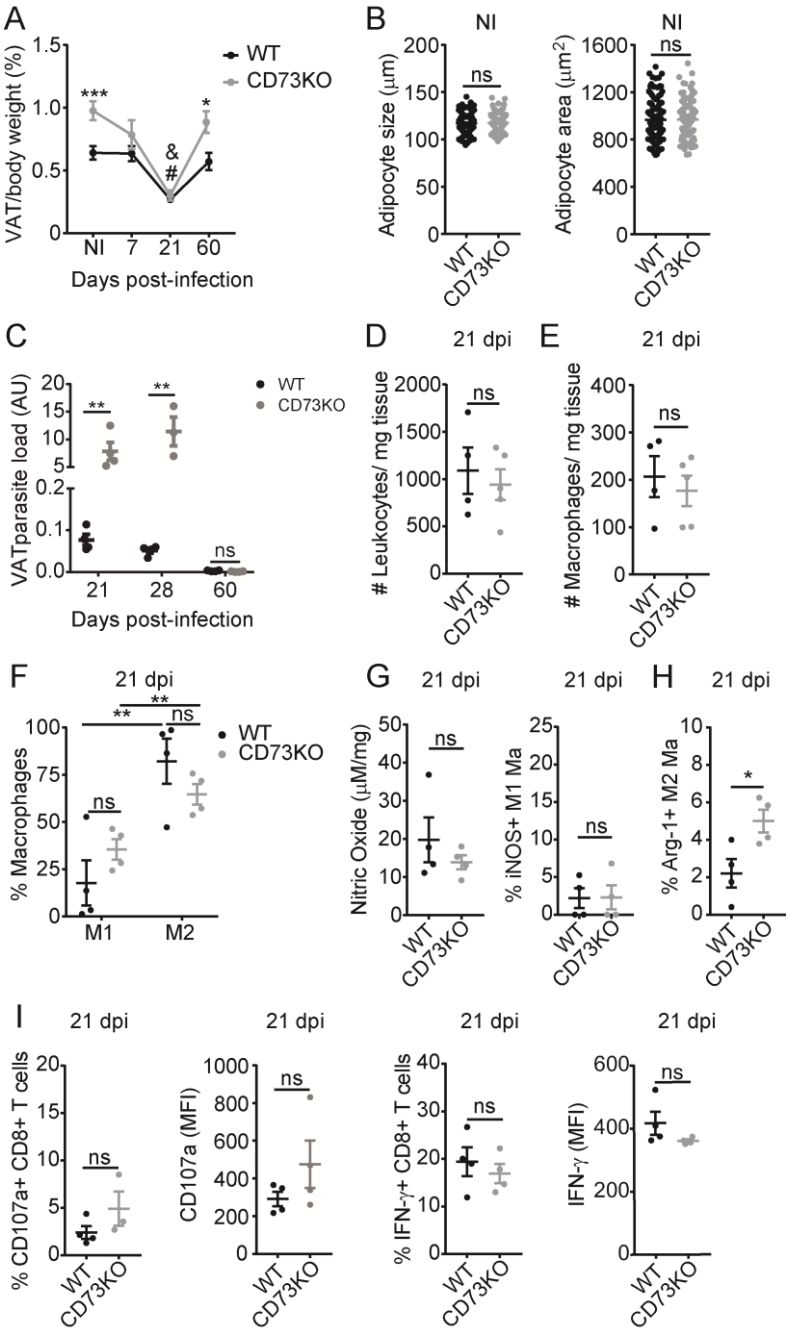

Figure 4. CD73KO mice showed increased VAT parasite burden. (A) Kinetics of VAT/body weight ratio in non-infected (NI) or infected WT (black line) and CD73KO (grey line) mice (n= 8-12) (& $p < 0.001$ NI *vs.* 21 dpi CD73KO and # $p < 0.01$ NI *vs.* 21 dpi WT). (B) Adipocyte size and area from non-infected (NI) WT (black) and CD73-deficient (grey) mice. (C) Quantitative assessment of VAT parasite burden kinetics by real-time PCR in WT and CD73KO mice (n=3-5). (D) Absolute number of VAT leukocytes and (E) VAT Ma normalized by milligram of tissue (n=4-5). (F) Relative percentage of Ma with M1 and M2 phenotype. Percentages are expressed as the relationship between both single positive populations (n=4). (G) NO levels measured by Griess reagent in infected VAT. Frequency of $iNOS^+$ M1-like Ma (n=4). (H) Frequencies of $Arg1^+$ M2-like Ma (n=4). (I) Frequencies and MFI of $CD107a^+$ and IFN- γ^+ $CD8^+$ T cells (n= 4 per group). (D-I) The assays were comparative between WT and CD73KO VAT at 21 dpi. The results are expressed as mean ± SEM of a representative assay of two independent experiments (* $p < 0.05$; ** $p < 0.01$; *** $p < 0.001$; ns: non-significant).

Deficiency of CD73 activity fails to generate an effective microbicidal response against *T. cruzi* in liver

Next we wonder to assess the influence of CD73 deficiency on immune cell profiles in liver, another known parasite reservoir [31]. As shown in Fig. 5A-B, no differences were observed in the liver/body weight ratio or in the absolute number of leukocytes within the tissue between both groups of mice at 21 dpi. At this time point, total number of hepatic macrophages raised in CD73KO compared to WT due to a higher frequency and absolute number of M1-like macrophages subset (Fig.5C-D). The frequency of $iNOS^+$ M1-like macrophages and hepatic NO levels were significantly reduced in CD73-deficient liver compared to WT, as shown in Fig. 5E. In contrast, no differences were found in the frequency of IL-12-producing M1-like macrophages (Fig. 5F), and in Arg-1^+ or IL-10^+ -M2-like macrophages in CD73KO liver compared to WT liver (Fig. 5G). Similarly, no differences were found in the frequency of total $CD8^+$ T cells, as well as in $CD107a^+$ and IFN-γ^+ -$CD8^+$ T cells (Fig. 5H).

Liver parasite load was markedly increased in CD73KO compared to WT mice at 21 dpi but at 28 and 60 dpi both groups of mice showed similar levels of parasite burden (Fig. 5I). In agreement, at 21 dpi CD73KO mice exhibited increased liver damage measured by plasma ALT and AST levels in comparison with WT mice. Strikingly, CD73KO mice exhibited increased liver injury markers also at 60 dpi (Fig. 5J). Altogether, these data suggest that in liver CD73 enzymatic deficiency is insufficient to set up an early effective microbicidal response required to keep the infection under control even though the macrophage polarization seem to occur.

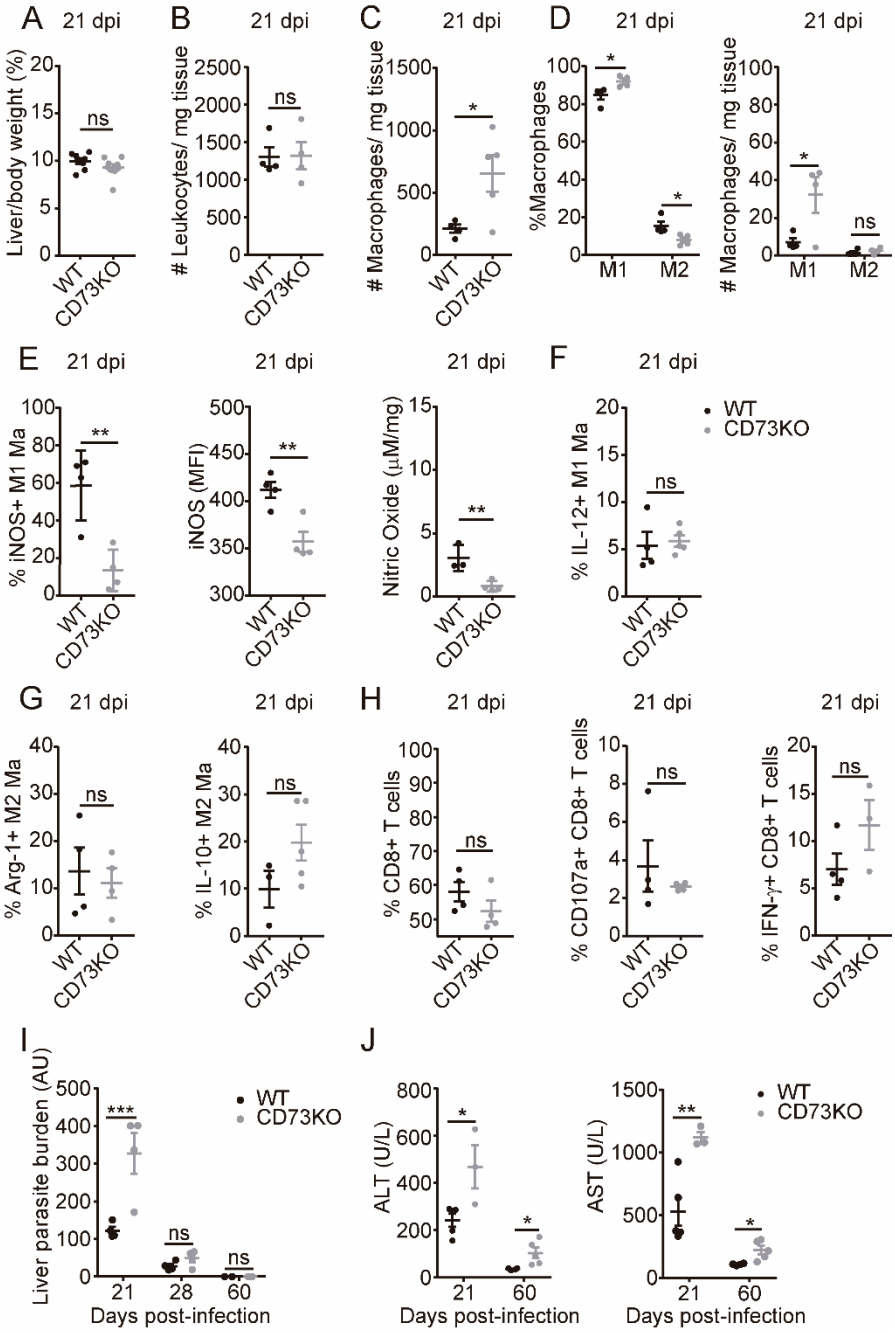

Figure 5. Deficiency of CD73 increased M1-like Ma in the liver but was insufficient to generate a microbicidal response against *T. cruzi*. (A) Liver/body weight ratio in infected WT (black) and CD73KO (grey) mice (n= 8). (B) Absolute number of leukocytes and (C) Ma normalized by milligram of tissue (n=4-5). (D) Relative percentage and absolute number of Ma with M1 and M2 phenotype normalized by milligram of liver tissue (n=4). (E) Frequency and MFI of iNOS expression in cells gated in M1 Ma phenotype (n= 4). Hepatic NO levels measured by Griess reagent (n=4). (F) Frequency of IL-12$^+$ M1 Ma (n=4-5). (G) Frequency of Arg-1$^+$ and IL-10$^+$ gated in M2 Ma (n= 4-5). (H) Frequencies of CD8$^+$ T cells, CD107a$^+$- and IFN-γ$^+$ CD8$^+$ T cells (n=4). (A-H) The assays were comparative between WT and CD73KO liver at 21 dpi. (I) Quantitative assessment of liver parasite burden kinetics by real-time PCR (n=3-5). (J) Plasma levels of aspartate aminotransferase (AST) and alanine aminotransaminase (ALT) at 21 and 60 dpi in WT and CD73KO mice (n=4-5). The results are expressed as mean ± SEM of a representative assay of at least two independent experiments if not indicated otherwise (* $p < 0.05$; ** $p < 0.01$; *** $p < 0.001$; ns: non-significant).

Deficiency of CD73 induces a tissue-dependent impact on ATP/ADO ratio

To further define the link between tissue-specific regulation of immune response to *T. cruzi* and CD73 deficiency, we established the ATP/ADO ratio released by each tissue after infection. To this aim, the organs or tissues were incubated in sterile PBS in a settled weight/volume ratio for 1h at 37°C and released ATP and ADO were quantified by bioluminescence assay or HPLC, respectively. We found a significantly higher amount of ATP and lower levels of ADO released by CD73KO hearts compared to WT hearts at 7 dpi (Fig. 6A-B). At this time point, no significant differences were found in ATP and ADO released by infected livers from both groups of mice. In contrast, CD73KO VAT secreted significant lower amount of ADO while no differences were observed in ATP levels compared to WT VAT. Notably, CD73-deficient tissues exhibited significantly higher ATP/ADO ratio than their WT counterparts, confirming that CD73 is determinant for the production of ADO in the context of this infection (Fig. 6C). Moreover, cardiac ATP/ADO ratio was 4.8 and 2.7 folds higher than CD73KO liver and VAT, respectively. The purinergic microenvironment remains skewed towards ATP in CD73KO cardiac tissue until 21 dpi (Fig. 6D). In contrast, CD73KO infected livers released higher amounts of ATP and ADO than the WT counterpart, while CD73KO VAT released higher levels of ATP with non-detectable levels of ADO at 21 dpi (Fig. 6D-E). These results suggest that CD73KO hearts exhibit an ATP/ADO ratio clearly biased toward an inflammatory milieu.

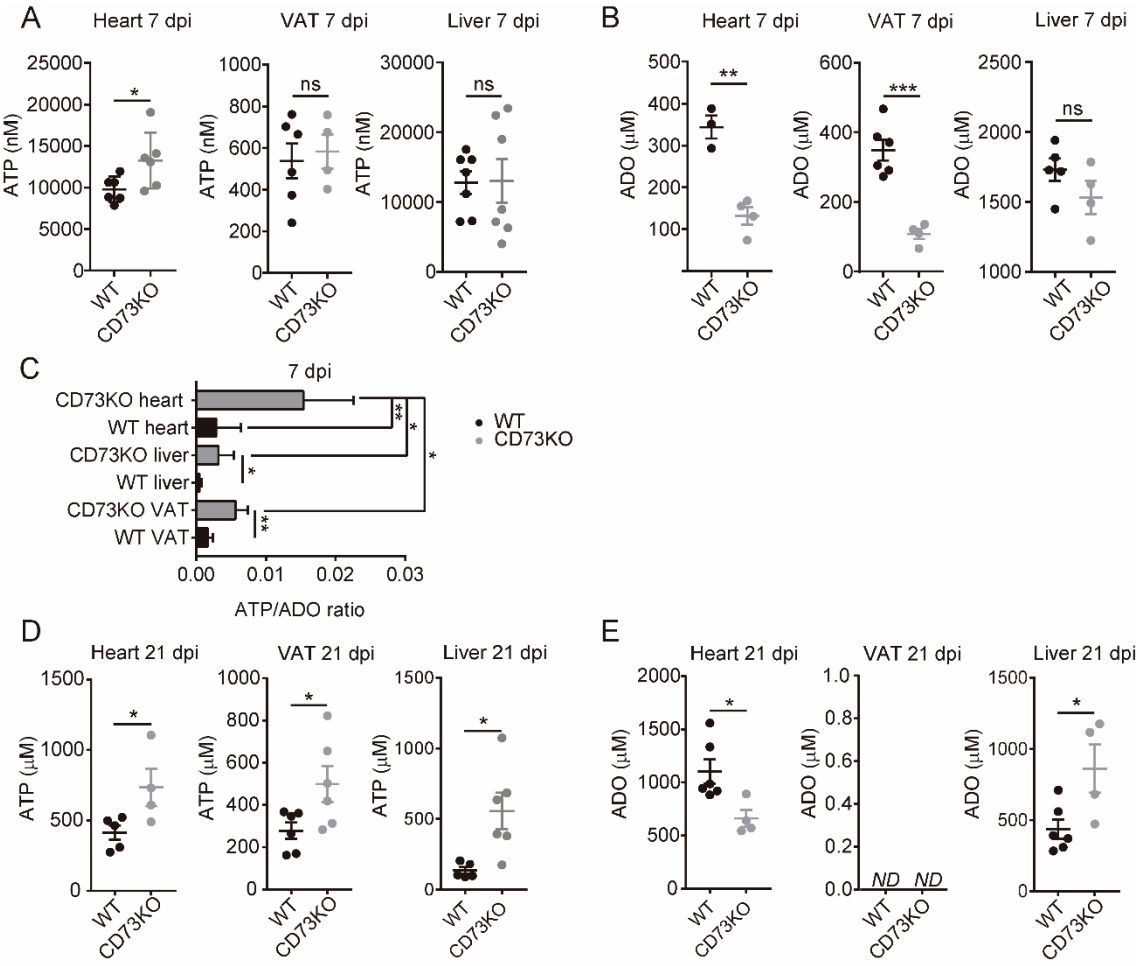

Figure 6. CD73 deficiency exhibits a tissue-dependent impact on ATP/ADO ratio. Each infected tissue was incubated in PBS for 1h at 37°C and the amount of ATP and ADO were measured in the supernatants through bioluminescent assay or HPLC, respectively. (A) ATP levels (n=6-7) and (B) ADO levels (n=4-6) in supernatants of hearts, VAT and livers in WT and CD73KO mice at 7 dpi. (C) ATP/ADO ratio determined at 7 dpi in paired samples obtained from the same mouse. Results are mean ± SEM and represent three independent experiments. (* $p < 0.05$; ** $p < 0.01$; *** $p < 0.001$; ns: non-significant). (D) ATP levels and (E) ADO levels in supernatants of hearts, livers and VAT in WT and CD73KO mice at 21 dpi (n=4-6). Results are mean ± SEM and represent two independent experiments.

We next determined the cellular source of CD73 ectoenzyme in each tissue. To this aim, the expression of CD73 ectoenzyme in immune cells and parenchymal cells was quantified at 7 dpi in WT tissues. Through immunofluorescence confocal assay we determined the MFI/cell by making a Z-projection of the stacks of confocal images in 10 HPF. The study revealed that although immune cells exhibited significantly higher levels of CD73 expression than parenchymal cells, cardiomyocytes, adipocytes and hepatocytes express low amount of this ectoenzyme (Fig. 7A). In addition, the expression level of CD39 and CD73 ectoenzymes in each leukocyte population was

assessed by FACS analysis at 21 dpi. As depicted in Fig. 7B, the predominant cell population in infected hearts were $CD4^+$ T cells followed by $CD8^+$ T cells, myeloid cells (macrophages and neutrophils) and $CD19^+$ cells (B lymphocytes). There were no significant differences among the frequencies of each leukocyte population in VAT, while in the liver only the percentage of B cells was lower than other immune cell populations. Within the heart and liver, macrophages and neutrophils are the main leukocyte populations expressing CD39 and CD73. In VAT, the entire T cell compartment expressed CD39 enzyme, while the expression of CD73 predominated in macrophages and neutrophils. The results strongly suggest that the unique purinergic environment generated in each analyzed tissue depends on the combinatory effect of ectoenzymes expressed in immune cells but also in parenchymal cells. However, further studies are necessary to establish the participation of each cell population.

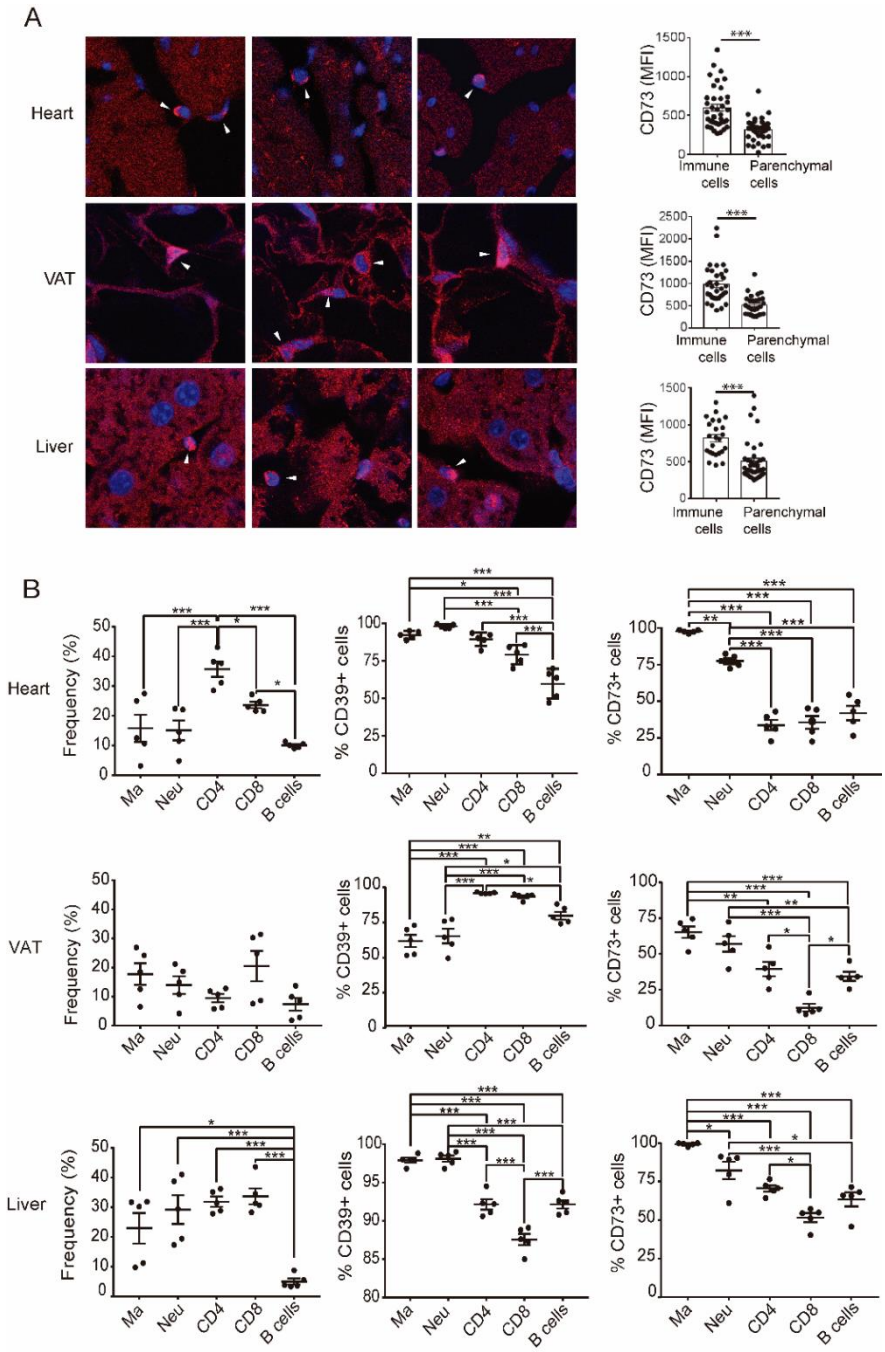

Figure 7. Cellular source of purinergic ectoenzymes. (A) Representative confocal images of CD73 immmunostainig in heart, VAT and liver at 7dpi obtained with the FLUOVIEW FV1200 Olympus confocal microscope (original magnification 60x plus 4x digital zoom). The arrowheads indicate immune cells. The mean fluorescence intensity (MFI) was quantified using Image J software by making a Z-projection of the stacks of confocal images and analyzing the mean grey value of the ROIs after the subtraction of fluorescence given by the secondary antibody and by the tissue autofluorescence. (B) Frequency of macrophages (Ma), neutrophils (Neu), CD3+ CD4+ T cells (CD4), CD3+ CD8+ T cells (CD8), and B cells and percentage of CD39+ and CD73+ cells among each leukocyte population in heart, VAT and liver from WT mice at 21 dpi (n=5). Leukocytes were previously gated in CD45+ cells. Results are mean ± SEM (* $p < 0.05$; ** $p < 0.01$; *** $p < 0.001$; ND: non detectable; ns: non-significant).

4. Discussion

Although CD73 on immune cells has emerged as a critical enzyme and therapeutic target in cardiovascular disorders [35-37], the participation of CD73/ADO purinergic pathway in the context of cardiac infection has been poorly investigated. The present study demonstrates that abrogation of CD73 enzymatic activity improves early local immune response against *T. cruzi* infection within the myocardium. However, the results obtained also highlight the fact that deficiency of CD73 activity modulates anti-*T. cruzi* response in a tissue-specific manner.

We have recently reported that transient pharmacologic inhibition of CD73 activity early after *T. cruzi* infection critically diminished cardiac parasite load by increasing M1 macrophages and by enhancing the local production of M1-related cytokines and microbicidal metabolites. Regarding acquired immune response, CD73 inhibition diminishes the frequency of CD4 T cells compatible with the development of type-1 regulatory T cell profile [19]. The overall response prevents the progression of the cardiomyopathy, suggesting that CD73 activity critically modulates cardiac immune response against *T. cruzi* infection. Notably, after a short period of time, the inflammatory and microbicidal milieu switches toward an anti-inflammatory environment that likely supports myocardial wound healing. In line with these observations, here we observed an important inflammatory and microbicidal response in the myocardium of CD73-deficient mice associated with a significant reduction in cardiac parasite load. The enhanced frequency of CD8+ T cells producing IFN-γ and expressing CD107a in CD73KO hearts may be controlling and reducing local parasite load. These findings are in line with previous studies, which revealed that ADO production inhibits the activation and TCR-triggered effector functions of CD8+ T cells [38-40]. Nevertheless, no significant differences were found in specific

biochemical marker of cardiac damage in both groups of mice, suggesting that the overall balance between increased parasite load in WT mice and potentiated inflammatory milieu observed in CD73KO mice, resulted in a comparable myocardial injury.

These findings suggest that inactivation of CD73 activity should represent an advantage to keep the acute infection under control. However, quite unexpectedly, parasitemia in deficient mice were significantly increased indicating that there was a favorable niche for parasite development outside the myocardium. Considering that adipose tissue has been postulated as an important reservoir for *T. cruzi* [41, 42], we thereby focused on VAT response. Strikingly, CD73KO mice exhibited higher basal VAT/body weight ratio and they released lower amounts of ADO from infected VAT than WT mice. These observations are in agreement with previous reports showing that genetic deletion of A1-ADO receptor, the predominant ADO receptor in white adipose tissue, is associated with an increased fat mass independent of the mouse strain [43, 44]. Furthermore, in line with these reports inactivation of CD73 promotes atherosclerotic plaque formation [45] and increases intra-myocellular lipid levels [46].

After infection, adipose tissue displays widespread macrophage invasion. The influx of innate immune cells is accompanied by an increased expression of lipolytic enzymes (hormone sensitive lipase –HSL- and lipoprotein lipase –LPL-), which lead to a reduction in fat mass [41]. This reduction can also be supported by inflammatory mediators released from local immune cells. Inflammatory cytokines, particularly TNF exhibits potent lipolytic activity [47], by increasing the expression of lipolytic enzymes [48] and decreasing the expression of many genes involved in preventing lipolysis [49-51]. In this sense, we found that M1 macrophages profile predominated over M2 macrophages during the acute phase within VAT from both groups of mice.

In contrast, during the chronic phase of the infection macrophages with M2 phenotype predominate over M1 [52]. On the other hand, it has been also reported that *T. cruzi* trypomastigotes enter preadipocytes and adipocytes through low-density lipoprotein receptors (LDLr), among others [53]. Therefore, it is plausible to think that parasite replication together with the inflammatory milieu established within adipose tissue could promote the reduction in VAT mass observed early after infection, but during the chronic phase the reestablishment of the anti-inflammatory M2 profile help to restore VAT weight to the original observed values.

In contrast to the strong immune response established in infected CD73-deficient myocardium, in VAT the number and frequency of macrophages with M1-phenotype do not differ between infected CD73-deficient and WT mice. Nevertheless, the increased frequency of Arg-1+ M2-like macrophages observed in CD73KO could be promoting the intracellular parasite growth, since Arg-1 expression is linked to *T. cruzi* parasite growth [54]. Moreover, parasite ectonucleotidases, such as CD39, could be hydrolyzing the increased ATP levels observed in CD73KO VAT and thus promoting parasite growth providing an advantage in its development over that hosted in WT VAT. In this sense, several studies suggest that the presence of ATP catabolizing ectoenzymes in microbes could modulate the host-pathogen interaction by positively influencing intracellular replication [55].

Similar to VAT immune response, in the liver $CD8^+$ T cells do not show differences between the two groups. Strikingly, although the amount of macrophages is increased in CD73-deficient liver and the frequency of M1-like macrophage profile is significantly higher than the WT counterpart, the frequency of hepatic M1-like macrophages producing Th1-inducing cytokines or M2-like macrophages producing IL-10 regulatory cytokine, do not significantly differ between both groups of mice. In

summary, the hyperplasia observed in CD73-deficient VAT in association with comparable microbicidal mechanisms triggered in VAT and liver from both experimental groups likely offer advantages for parasite development in these *T. cruzi* target tissues. Thus, the more permissive environment coupled with augmented parasitemia supported the increased parasite load observed in CD73-deficient VAT and liver. However, it still remains to be investigated if other immune mechanisms, not analyzed in this work, could also be favoring parasite replication in the setting of CD73-deficiency within these tissues.

The release of adenine nucleotides to the extracellular milieu represents a critical first step for the initiation of purinergic signaling. Once released, the half-life in the extracellular milieu is critically determined by the activity of ATP metabolic enzymes [10, 56], and the final effects on the innate and adaptive immune response depend on the balance between ATP and ADO in the microenvironment of the cells [4, 57]. Regarding the influence of ATP metabolic enzymes in cardiac settings, it was recently described that CD73KO mice exhibit impaired cardiac function after ischemia/reperfusion since CD73 activity is determinant for the cardiac wound healing process after myocardial infarction. The underlying mechanism involves a profound increase in the hydrolysis of ATP/NAD and AMP, resulting primarily from CD73 activity but is independent of CD39 activity [58]. In the present work, we found that while the amount of ATP released at 7dpi by CD73-deficient infected hearts was significantly higher than their WT counterpart, the amount of ATP released by VAT and livers did not show differences among both groups of mice likely due to the fact that cardiac cells have a greater capacity to produce ATP than other parenchymal cells, as a consequence of their physiological function. Notably, ATP/ADO ratio from infected CD73KO hearts was significantly higher than the WT counterpart but also

than livers and VAT from CD73-deficient mice. Furthermore, the livers as well as VAT from CD73KO mice exhibited increased ATP/ADO ratio in comparison with the corresponding tissues from WT mice. The differences observed in the local immune responses may be due, at least in part, to the differential expression of purinergic enzymes that lead to a unique extracellular purinergic microenvironment in each tissue. However, it has been reported that cells that inhabit the tissues must metabolically adapt to their microenvironment and develop transcriptional signatures that reflect adaptation to function within that tissue, so a metabolic fine tuning as a feature of niche adaptation cannot be entirely ruled out [59].

Our results clearly evidence that CD73 deficiency has a particular impact on host local immune response in infected hearts over other evaluated tissues. The increased availability of pro-inflammatory ATP combined with lower ADO levels within the myocardium deprived from CD73 activity could be determining the fate in the efficiency of anti-*T. cruzi* response observed in this clinically relevant target tissue. The results are relevant considering the increasing number of reports that propose targeting purinergic pathways as therapeutic approaches for diverse pathologies from cancer to myocardial infarction. In this sense, few investigations have addressed the impact of CD73 abrogation in individual tissues in the setting of a systemic inflammation.

5. Conclusion

Our results demonstrate that breaking ATP catabolic machinery by inhibiting the enzymatic activity of CD73 ectoenzyme generates a unique purinergic milieu within each target tissue that contributed to the modulation of host immune response which modifies parasite-host interaction and, consequently, *T. cruzi* persistence. In this sense

it is important to stress that tissue parasite load did not exhibit differences at later times after infection suggesting that the immune response is effective in determine the final clearance of the parasite independent of the tissue. The effects of CD73 deficiency in the chronic phase of the cardiomyopathy are under investigation in our laboratory. Considering the intense studies currently conducting to postulate purinergic signaling as possible therapeutic target, our results alert on the differential impact that purinergic system exhibits on each particular tissue.

6. Footnotes:

Abbreviations used in this article: ADO, adenosine; ATP, adenosine triphosphate; CD39, ectonucleoside triphosphate diphosphohydrolase-1 enzyme; CD73, ecto-5′-nucleotidase enzyme; AMP, adenosine monophosphate; Mo, monocytes; Ma, macrophages; NO, nitric oxide; iNOS, inducible nitric oxide synthase; VAT, visceral adipose tissue; WT,: wild-type; dpi, days post-infection; MFI, mean fluorescence intensity; SVF, stromal vascular fraction; FACS, Fluorescence-activated cell sorting; KO, knock out; APCP, adenosine 5′α, β-methylene-diphosphate; IL, interleukin; CK, creatine kinase; Ly6C, lymphocyte antigen 6 complex; FSC-H, forward light scatter-height; FSC-A, forward light scatter-area; ROIs, regions of interest.

Fundings: This work was supported by Secretaría de Ciencia y Tecnología, Universidad Nacional de Córdoba (113/17), Agencia Nacional de Promoción Científica y Tecnológica (ANPCyT) Fondo para la Investigación Científica y Tecnológica (PICT 2013-2885 and 2015-1130), Consejo Nacional de Investigaciones Científicas y Técnicas (CONICET) (PIP11220120100620), and by Ministerio de Ciencia y Tecnología, Gobierno de la Provincia de Córdoba (1143/10). MGT and MPA are members of the scientific and technical career from the Consejo Nacional de Investigaciones Científicas y Técnicas de la República Argentina (CONICET). NEP, LMS, MCG, GB and NE thanks CONICET for the fellowships granted. NEP also thanks fellowships granted from ANPCyT-FONCyT and CONICET.

Authorship contribution: Conceived and designed the experiments: NE, LMS, NEP, GB, RCC and MPA. Performed the experiments: NE, LMS, GB, MGT, MCG, MPA. Analyzed the data: NE, LMS, GB, NEP and MPA. Wrote the paper: NE and MPA.

Acknowledgments: We are grateful to Dr. Cinthia Stempin for reagents donation. We thank Dra. Pilar Crespo, Dr. Carlos Mas, Dra. Paula Abadie, Alejandra Romero, Dra. Laura Gatica, Dra. Cecilia Sampedro, Victoria Blanco, Dra. Soledad Miró, Diego Lutti and Fabricio Navarro for their skillful technical assistance.

7. References

[1] C. Cekic, J. Linden, Purinergic regulation of the immune system, Nature Reviews. Immunology, 16 (2016) 177-192. doi: 10.1038/nri.2016.4
[2] M.R. Bono, D. Fernandez, F. Flores-Santibanez, M. Rosemblatt, D. Sauma, CD73 and CD39 ectonucleotidases in T cell differentiation: Beyond immunosuppression, FEBS letters, 589 (2015) 3454-3460. doi: 10.1016/j.febslet.2015.07.027
[3] B. Csoka, Z.H. Nemeth, L. Virag, P. Gergely, S.J. Leibovich, P. Pacher, C.X. Sun, M.R. Blackburn, E.S. Vizi, E.A. Deitch, G. Hasko, A2A adenosine receptors and C/EBPbeta are crucially required for IL-10 production by macrophages exposed to Escherichia coli, Blood, 110 (2007) 2685-2695. doi: 10.1182/blood-2007-01-065870
[4] L. Antonioli, P. Pacher, E.S. Vizi, G. Hasko, CD39 and CD73 in immunity and inflammation, Trends in Molecular Medicine, 19 (2013) 355-367. doi: 10.1016/j.molmed.2013.03.005
[5] L. Antonioli, C. Blandizzi, P. Pacher, G. Hasko, Immunity, inflammation and cancer: a leading role for adenosine, Nature Reviews. Cancer, 13 (2013) 842-857. doi: 10.1038/nrc3613
[6] F. Di Virgilio, E. Adinolfi, Extracellular purines, purinergic receptors and tumor growth, Oncogene, 36 (2017) 293-303. doi: 10.1038/onc.2016.206
[7] G. Forte, R. Sorrentino, A. Montinaro, A. Luciano, I.M. Adcock, P. Maiolino, C. Arra, C. Cicala, A. Pinto, S. Morello, Inhibition of CD73 improves B cell-mediated anti-tumor immunity in a mouse model of melanoma, Journal of Immunology, 189 (2012) 2226-2233. doi: 10.4049/jimmunol.1200744
[8] J. Stagg, U. Divisekera, H. Duret, T. Sparwasser, M.W. Teng, P.K. Darcy, M.J. Smyth, CD73-deficient mice have increased antitumor immunity and are resistant to experimental metastasis, Cancer Research, 71 (2011) 2892-2900. doi: 10.1158/0008-5472.CAN-10-4246
[9] G. Hasko, B. Csoka, B. Koscso, R. Chandra, P. Pacher, L.F. Thompson, E.A. Deitch, Z. Spolarics, L. Virag, P. Gergely, R.H. Rolandelli, Z.H. Nemeth, Ecto-5'-nucleotidase (CD73) decreases mortality and organ injury in sepsis, Journal of Immunology, 187 (2011) 4256-4267. doi: 10.4049/jimmunol.1003379
[10] P. Wan, X. Liu, Y. Xiong, Y. Ren, J. Chen, N. Lu, Y. Guo, A. Bai, Extracellular ATP mediates inflammatory responses in colitis via P2 x 7 receptor signaling, Scientific Reports, 6 (2016) 19108. doi: 10.1038/srep19108
[11] M.S. Alam, J.L. Kuo, P.B. Ernst, V. Derr-Castillo, M. Pereira, D. Gaines, M. Costales, E. Bigley, K. Williams, Ecto-5'-nucleotidase (CD73) regulates host inflammatory responses and exacerbates murine salmonellosis, Scientific Reports, 4 (2014) 4486. doi: 10.1038/srep04486
[12] V. Francois, H. Shehade, V. Acolty, N. Preyat, P. Delree, M. Moser, G. Oldenhove, Intestinal immunopathology is associated with decreased CD73-generated adenosine during lethal infection, Mucosal immunology, 8 (2015) 773-784. doi: 10.1038/mi.2014.108
[13] D.A. Mahamed, L.E. Toussaint, M.S. Bynoe, CD73-generated adenosine is critical for immune regulation during Toxoplasma gondii infection, Infection and Immunity, 83 (2015) 721-729. doi: 10.1128/IAI.02536-14
[14] P. Chrobak, R. Charlebois, P. Rejtar, R. El Bikai, B. Allard, J. Stagg, CD73 plays a protective role in collagen-induced arthritis, Journal of Immunology, 194 (2015) 2487-2492. doi: 10.4049/jimmunol.1401416
[15] A.N. Samudra, K.M. Dwyer, C. Selan, S. Freddi, L. Murray-Segal, M. Nikpour, M.J. Hickey, K. Peter, S.C. Robson, M. Sashindranath, P.J. Cowan, H.H. Nandurkar, CD39 and CD73 activity are protective in a mouse model of antiphospholipid antibody-induced miscarriages, Journal of Autoimmunity, (2017). doi: 10.1016/j.jaut.2017.10.009
[16] F.S. Machado, K.M. Tyler, F. Brant, L. Esper, M.M. Teixeira, H.B. Tanowitz, Pathogenesis of Chagas disease: time to move on, Frontiers in Bioscience, 4 (2012) 1743-1758.
[17] R.F. Zanin, E. Braganhol, L.S. Bergamin, L.F. Campesato, A.Z. Filho, J.C. Moreira, F.B. Morrone, J. Sevigny, M.R. Schetinger, A.T. de Souza Wyse, A.M. Battastini, Differential macrophage activation alters the expression profile of NTPDase and ecto-5'-nucleotidase, PloS One, 7 (2012) e31205. doi: 10.1371/journal.pone.0031205

[18] B. Csoka, Z. Selmeczy, B. Koscso, Z.H. Nemeth, P. Pacher, P.J. Murray, D. Kepka-Lenhart, S.M. Morris, Jr., W.C. Gause, S.J. Leibovich, G. Hasko, Adenosine promotes alternative macrophage activation via A2A and A2B receptors, FASEB Journal : official publication of the Federation of American Societies for Experimental Biology, 26 (2012) 376-386. doi: 10.1096/fj.11-190934
[19] N.E. Ponce, L.M. Sanmarco, N. Eberhardt, M.C. Garcia, H.W. Rivarola, R.C. Cano, M.P. Aoki, CD73 Inhibition Shifts Cardiac Macrophage Polarization toward a Microbicidal Phenotype and Ameliorates the Outcome of Experimental Chagas Cardiomyopathy, Journal of Immunology, 197 (2016) 814-823. doi: 10.4049/jimmunol.1600371
[20] N.E. Ponce, R.C. Cano, E.A. Carrera-Silva, A.P. Lima, S. Gea, M.P. Aoki, Toll-like receptor-2 and interleukin-6 mediate cardiomyocyte protection from apoptosis during *Trypanosoma cruzi* murine infection, Medical Microbiology and Immunology, 201 (2012) 145-155. doi: 10.1007/s00430-011-0216-z
[21] L.M. Sanmarco, N. Eberhardt, N.E. Ponce, R.C. Cano, G. Bonacci, M.P. Aoki, New Insights into the Immunobiology of Mononuclear Phagocytic Cells and Their Relevance to the Pathogenesis of Cardiovascular Diseases, Frontiers in Immunology, 8 (2017) 1921. doi: 10.3389/fimmu.2017.01921
[22] N.E. Ponce, E.A. Carrera-Silva, A.V. Pellegrini, S.I. Cazorla, E.L. Malchiodi, A.P. Lima, S. Gea, M.P. Aoki, *Trypanosoma cruzi*, the causative agent of Chagas disease, modulates interleukin-6-induced STAT3 phosphorylation via gp130 cleavage in different host cells, Biochimica et Biophysica Acta, 1832 (2013) 485-494. doi: 10.1016/j.bbadis.2012.12.003
[23] L.M. Sanmarco, N.E. Ponce, L.M. Visconti, N. Eberhardt, M.G. Theumer, A.R. Minguez, M.P. Aoki, IL-6 promotes M2 macrophage polarization by modulating purinergic signaling and regulates the lethal release of nitric oxide during *Trypanosoma cruzi* infection, Biochimica et Biophysica Acta, 1863 (2017) 857-869. doi: 10.1016/j.bbadis.2017.01.006
[24] P. Aoki Mdel, R.C. Cano, A.V. Pellegrini, T. Tanos, N.L. Guinazu, O.A. Coso, S. Gea, Different signaling pathways are involved in cardiomyocyte survival induced by a *Trypanosoma cruzi* glycoprotein, Microbes and Infection, 8 (2006) 1723-1731. doi: 10.1016/j.micinf.2006.02.010
[25] M.P. Aoki, N.L. Guinazu, A.V. Pellegrini, T. Gotoh, D.T. Masih, S. Gea, Cruzipain, a major *Trypanosoma cruzi* antigen, promotes arginase-2 expression and survival of neonatal mouse cardiomyocytes, American journal of physiology. Cell physiology, 286 (2004) C206-212. doi: 10.1152/ajpcell.00282.2003
[26] R.L. Tarleton, Parasite persistence in the aetiology of Chagas disease, International Journal for Parasitology, 31 (2001) 550-554.
[27] F.S. Machado, W.O. Dutra, L. Esper, K.J. Gollob, M.M. Teixeira, S.M. Factor, L.M. Weiss, F. Nagajyothi, H.B. Tanowitz, N.J. Garg, Current understanding of immunity to *Trypanosoma cruzi* infection and pathogenesis of Chagas disease, Seminars in Immunopathology, 34 (2012) 753-770. doi: 10.1007/s00281-012-0351-7
[28] F. Nagajyothi, M.S. Desruisseaux, L.M. Weiss, S. Chua, C. Albanese, F.S. Machado, L. Esper, M.P. Lisanti, M.M. Teixeira, P.E. Scherer, H.B. Tanowitz, Chagas disease, adipose tissue and the metabolic syndrome, Memorias do Instituto Oswaldo Cruz, 104 Suppl 1 (2009) 219-225.
[29] L.F. Thompson, H.K. Eltzschig, J.C. Ibla, C.J. Van De Wiele, R. Resta, J.C. Morote-Garcia, S.P. Colgan, Crucial role for ecto-5'-nucleotidase (CD73) in vascular leakage during hypoxia, The Journal of Experimental Medicine, 200 (2004) 1395-1405. doi: 10.1084/jem.20040915
[30] S.D. Parlee, S.I. Lentz, H. Mori, O.A. MacDougald, Quantifying size and number of adipocytes in adipose tissue, Methods in Enzymology, 537 (2014) 93-122. doi: 10.1016/B978-0-12-411619-1.00006-9
[31] E.A. Carrera-Silva, R.C. Cano, N. Guinazu, M.P. Aoki, A. Pellegrini, S. Gea, TLR2, TLR4 and TLR9 are differentially modulated in liver lethally injured from BALB/c and C57BL/6 mice during *Trypanosoma cruzi* acute infection, Molecular Immunology, 45 (2008) 3580-3588. doi: 10.1016/j.molimm.2008.05.004

[32] M. Piron, R. Fisa, N. Casamitjana, P. López-Chejade, L. Puig, M. Vergés, J. Gascón, J.G. i Prat, M. Portús, S. Sauleda, Development of a real-time PCR assay for *Trypanosoma cruzi* detection in blood samples, Acta Tropica, 103 (2007) 195-200.
[33] S.J. Koo, I.H. Chowdhury, B. Szczesny, X. Wan, N.J. Garg, Macrophages Promote Oxidative Metabolism To Drive Nitric Oxide Generation in Response to *Trypanosoma cruzi*, Infection and Immunity, 84 (2016) 3527-3541. doi: 10.1128/IAI.00809-16
[34] F. Nagajyothi, F.S. Machado, B.A. Burleigh, L.A. Jelicks, P.E. Scherer, S. Mukherjee, M.P. Lisanti, L.M. Weiss, N.J. Garg, H.B. Tanowitz, Mechanisms of *Trypanosoma cruzi* persistence in Chagas disease, Cellular Microbiology, 14 (2012) 634-643. doi: 10.1111/j.1462-5822.2012.01764.x
[35] F. Bonner, N. Borg, C. Jacoby, S. Temme, Z. Ding, U. Flogel, J. Schrader, Ecto-5'-nucleotidase on immune cells protects from adverse cardiac remodeling, Circulation Research, 113 (2013) 301-312. doi: 10.1161/CIRCRESAHA.113.300180
[36] G. Burnstock, Purinergic Signaling in the Cardiovascular System, Circulation Research, 120 (2017) 207-228. doi: 10.1161/CIRCRESAHA.116.309726
[37] G. Burnstock, Purinergic Signalling: Therapeutic Developments, Frontiers in Pharmacology, 8 (2017) 661. doi: 10.3389/fphar.2017.00661
[38] C. Sorrentino, F. Hossain, P.C. Rodriguez, R.A. Sierra, A. Pannuti, B.A. Osborne, L.M. Minter, L. Miele, S. Morello, Adenosine A2A Receptor Stimulation Inhibits TCR-Induced Notch1 Activation in CD8+T-Cells, Frontiers in Immunology, 10 (2019) 162. doi: 10.3389/fimmu.2019.00162
[39] M. Koshiba, H. Kojima, S. Huang, S. Apasov, M.V. Sitkovsky, Memory of extracellular adenosine A2A purinergic receptor-mediated signaling in murine T cells, The Journal of Biological Chemistry, 272 (1997) 25881-25889. doi: 10.1074/jbc.272.41.25881
[40] C. Linnemann, F.A. Schildberg, A. Schurich, L. Diehl, S.I. Hegenbarth, E. Endl, S. Lacher, C.E. Muller, J. Frey, L. Simeoni, B. Schraven, D. Stabenow, P.A. Knolle, Adenosine regulates CD8 T-cell priming by inhibition of membrane-proximal T-cell receptor signalling, Immunology, 128 (2009) e728-737. doi: 10.1111/j.1365-2567.2009.03075.x
[41] F. Nagajyothi, M.S. Desruisseaux, F.S. Machado, R. Upadhya, D. Zhao, G.J. Schwartz, M.M. Teixeira, C. Albanese, M.P. Lisanti, S.C. Chua, Jr., L.M. Weiss, P.E. Scherer, H.B. Tanowitz, Response of adipose tissue to early infection with *Trypanosoma cruzi* (Brazil strain), The Journal of Infectious Diseases, 205 (2012) 830-840. doi: 10.1093/infdis/jir840
[42] A.V. Ferreira, M. Segatto, Z. Menezes, A.M. Macedo, C. Gelape, L. de Oliveira Andrade, F. Nagajyothi, P.E. Scherer, M.M. Teixeira, H.B. Tanowitz, Evidence for *Trypanosoma cruzi* in adipose tissue in human chronic Chagas disease, Microbes and Infection, 13 (2011) 1002-1005. doi: 10.1016/j.micinf.2011.06.002
[43] R. Faulhaber-Walter, W. Jou, D. Mizel, L. Li, J. Zhang, S.M. Kim, Y. Huang, M. Chen, J.P. Briggs, O. Gavrilova, J.B. Schnermann, Impaired glucose tolerance in the absence of adenosine A1 receptor signaling, Diabetes, 60 (2011) 2578-2587. doi: 10.2337/db11-0058
[44] S.M. Johansson, E. Lindgren, J.N. Yang, A.W. Herling, B.B. Fredholm, Adenosine A1 receptors regulate lipolysis and lipogenesis in mouse adipose tissue-interactions with insulin, European Journal of Pharmacology, 597 (2008) 92-101. doi: 10.1016/j.ejphar.2008.08.022
[45] A. Buchheiser, A. Ebner, S. Burghoff, Z. Ding, M. Romio, C. Viethen, A. Lindecke, K. Kohrer, J.W. Fischer, J. Schrader, Inactivation of CD73 promotes atherogenesis in apolipoprotein E-deficient mice, Cardiovascular Research, 92 (2011) 338-347. doi: 10.1093/cvr/cvr218
[46] S. Burghoff, U. Flogel, S. Bongardt, V. Burkart, H. Sell, S. Tucci, K. Ikels, D. Eberhard, M. Kern, N. Kloting, J. Eckel, J. Schrader, Deletion of CD73 promotes dyslipidemia and intramyocellular lipid accumulation in muscle of mice, Archives of Physiology and Biochemistry, 119 (2013) 39-51. doi: 10.3109/13813455.2012.755547
[47] W.P. Cawthorn, J.K. Sethi, TNF-alpha and adipocyte biology, FEBS letters, 582 (2008) 117-131. doi: 10.1016/j.febslet.2007.11.051
[48] M.J. Lee, S.K. Fried, Glucocorticoids antagonize tumor necrosis factor-alpha-stimulated lipolysis and resistance to the antilipolytic effect of insulin in human adipocytes, American

Journal of Physiology. Endocrinology and metabolism, 303 (2012) E1126-1133. doi: 10.1152/ajpendo.00228.2012
[49] M. Ryden, A. Dicker, V. van Harmelen, H. Hauner, M. Brunnberg, L. Perbeck, F. Lonnqvist, P. Arner, Mapping of early signaling events in tumor necrosis factor-alpha -mediated lipolysis in human fat cells, The Journal of Biological Chemistry, 277 (2002) 1085-1091. doi: 10.1074/jbc.M109498200
[50] H.H. Zhang, M. Halbleib, F. Ahmad, V.C. Manganiello, A.S. Greenberg, Tumor necrosis factor-alpha stimulates lipolysis in differentiated human adipocytes through activation of extracellular signal-related kinase and elevation of intracellular cAMP, Diabetes, 51 (2002) 2929-2935.
[51] S.C. Souza, M.T. Yamamoto, M.D. Franciosa, P. Lien, A.S. Greenberg, BRL 49653 blocks the lipolytic actions of tumor necrosis factor-alpha: a potential new insulin-sensitizing mechanism for thiazolidinediones, Diabetes, 47 (1998) 691-695.
[52] M.E. Cabalen, M.F. Cabral, L.M. Sanmarco, M.C. Andrada, L.I. Onofrio, N.E. Ponce, M.P. Aoki, S. Gea, R.C. Cano, Chronic *Trypanosoma cruzi* infection potentiates adipose tissue macrophage polarization toward an anti-inflammatory M2 phenotype and contributes to diabetes progression in a diet-induced obesity model, Oncotarget, 7 (2016) 13400-13415. doi: 10.18632/oncotarget.7630
[53] F. Nagajyothi, L.M. Weiss, D.L. Silver, M.S. Desruisseaux, P.E. Scherer, J. Herz, H.B. Tanowitz, *Trypanosoma cruzi* utilizes the host low density lipoprotein receptor in invasion, PLoS Neglected Tropical Diseases, 5 (2011) e953. doi: 10.1371/journal.pntd.0000953
[54] C.C. Stempin, L.R. Dulgerian, V.V. Garrido, F.M. Cerban, Arginase in parasitic infections: macrophage activation, immunosuppression, and intracellular signals, Journal of Biomedicine & Biotechnology, 2010 (2010) 683485. doi: 10.1155/2010/683485
[55] F.M. Sansom, S.C. Robson, E.L. Hartland, Possible effects of microbial ecto-nucleoside triphosphate diphosphohydrolases on host-pathogen interactions, Microbiology and molecular biology reviews : MMBR, 72 (2008) 765-781. doi: 10.1128/MMBR.00013-08
[56] M. Idzko, D. Ferrari, H.K. Eltzschig, Nucleotide signalling during inflammation, Nature, 509 (2014) 310-317. doi: 10.1038/nature13085
[57] G. Hasko, B.N. Cronstein, Adenosine: an endogenous regulator of innate immunity, Trends in Immunology, 25 (2004) 33-39.
[58] N. Borg, C. Alter, N. Gorldt, C. Jacoby, Z. Ding, B. Steckel, C. Quast, F. Bonner, D. Friebe, S. Temme, U. Flogel, J. Schrader, CD73 on T Cells Orchestrates Cardiac Wound Healing After Myocardial Infarction by Purinergic Metabolic Reprogramming, Circulation, 136 (2017) 297-313. doi: 10.1161/CIRCULATIONAHA.116.023365
[59] G. Caputa, A. Castoldi, E.J. Pearce, Metabolic adaptations of tissue-resident immune cells, Nature Immunology, 20 (2019) 793-801. doi: 10.1038/s41590-019-0407-0

Highlights:

- CD73 ectoenzyme modulates ATP/ADO balance in each infection target tissue.
- ATP/ADO balance determines anti-*T. cruzi* response in a tissue-dependent manner.
- Immune cells within infected tissues express high levels of CD73 ectoenzyme.
- CD73 inhibition generates an efficient anti-T. cruzi response in cardiac tissue.
- CD73 deficiency fosters a favorable environment for parasite growth in VAT and liver.